Widespread changes in the posttranscriptional landscape at the Drosophila oocyte-to-embryo transition

Iva Kronja, Bingbing Yuan, Stephen Eichhorn, Kristina Dzeyk,

Jeroen Krijgsveld, David P. Bartel and Terry L. Orr-Weaver

Figure S1.

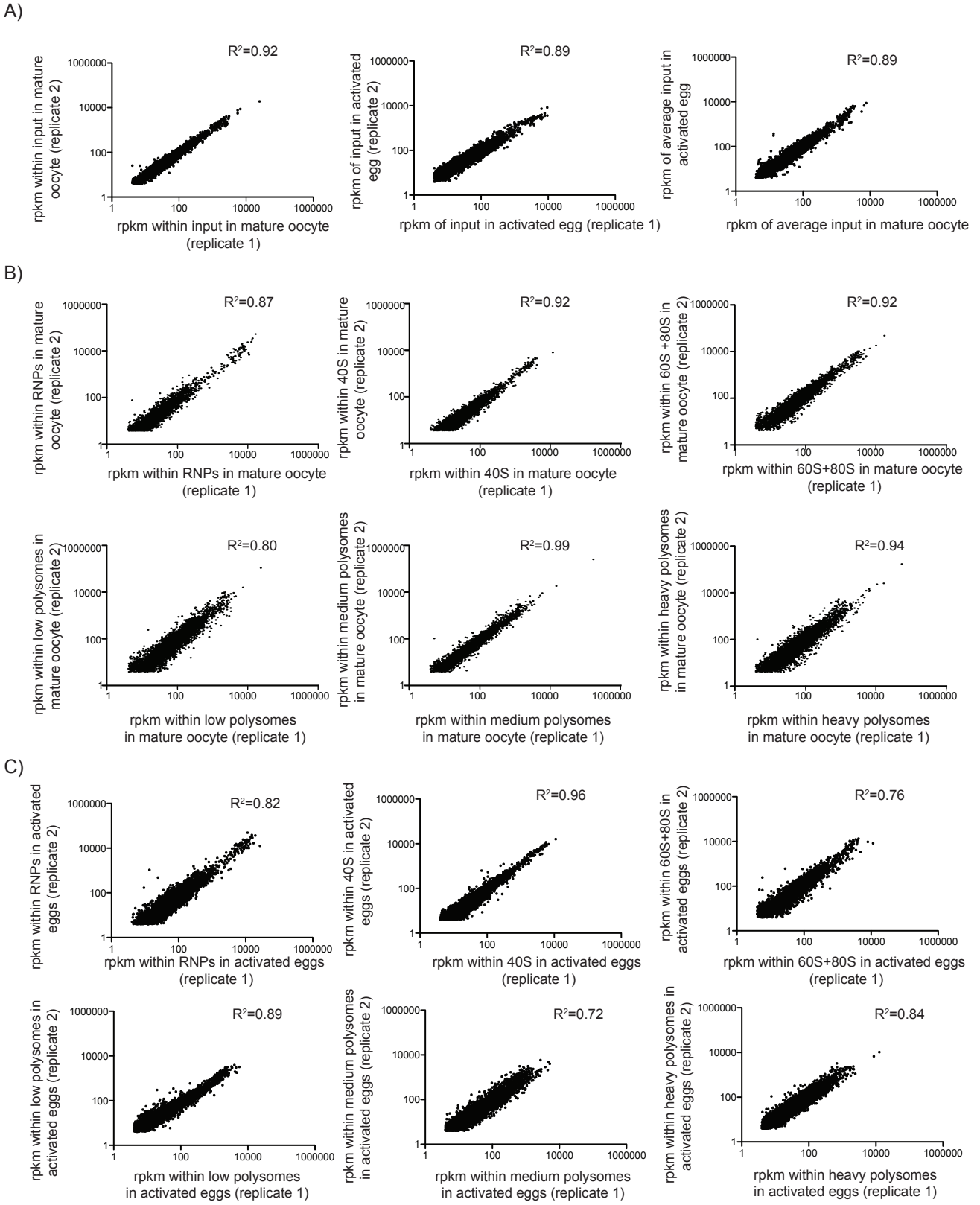
A)
R²=0.92
rpkm within input in mature oocyte (replicate 2)
rpkm within input in mature oocyte (replicate 1)
R²=0.89
rpkm of input in activated egg (replicate 2)
rpkm of input in activated egg (replicate 1)
R²=0.89
rpkm of average input in activated egg
rpkm of average input in mature oocyte
B)
R²=0.87
rpkm within RNPs in mature oocyte (replicate 2)
rpkm within RNPs in mature oocyte (replicate 1)
R²=0.92
rpkm within 40S in mature oocyte (replicate 2)
rpkm within 40S in mature oocyte (replicate 1)
R²=0.92
rpkm within 60S +80S in mature oocyte (replicate 2)
rpkm within 60S+80S in mature oocyte (replicate 1)
R²=0.80
rpkm within low polysomes in mature oocyte (replicate 2)
rpkm within low polysomes in mature oocyte (replicate 1)
R²=0.99
rpkm within medium polysomes in mature oocyte (replicate 2)
rpkm within medium polysomes in mature oocyte (replicate 1)
R²=0.94
rpkm within heavy polysomes in mature oocyte (replicate 2)
rpkm within heavy polysomes in mature oocyte (replicate 1)
C)
R²=0.82
rpkm within RNPs in activated eggs (replicate 2)
rpkm within RNPs in activated eggs (replicate 1)
R²=0.96
rpkm within 40S in activated eggs (replicate 2)
rpkm within 40S in activated eggs (replicate 1)
R²=0.76
rpkm within 60S+80S in activated eggs (replicate 2)
rpkm within 60S+80S in activated eggs (replicate 1)
R²=0.89
rpkm within low polysomes in activated eggs (replicate 2)
rpkm within low polysomes in activated eggs (replicate 1)
R²=0.72
rpkm within medium polysomes in activated eggs (replicate 2)
rpkm within medium polysomes in activated eggs (replicate 1)
R²=0.84
rpkm within heavy polysomes in activated eggs (replicate 2)
rpkm within heavy polysomes in activated eggs (replicate 1)

Figure S2.

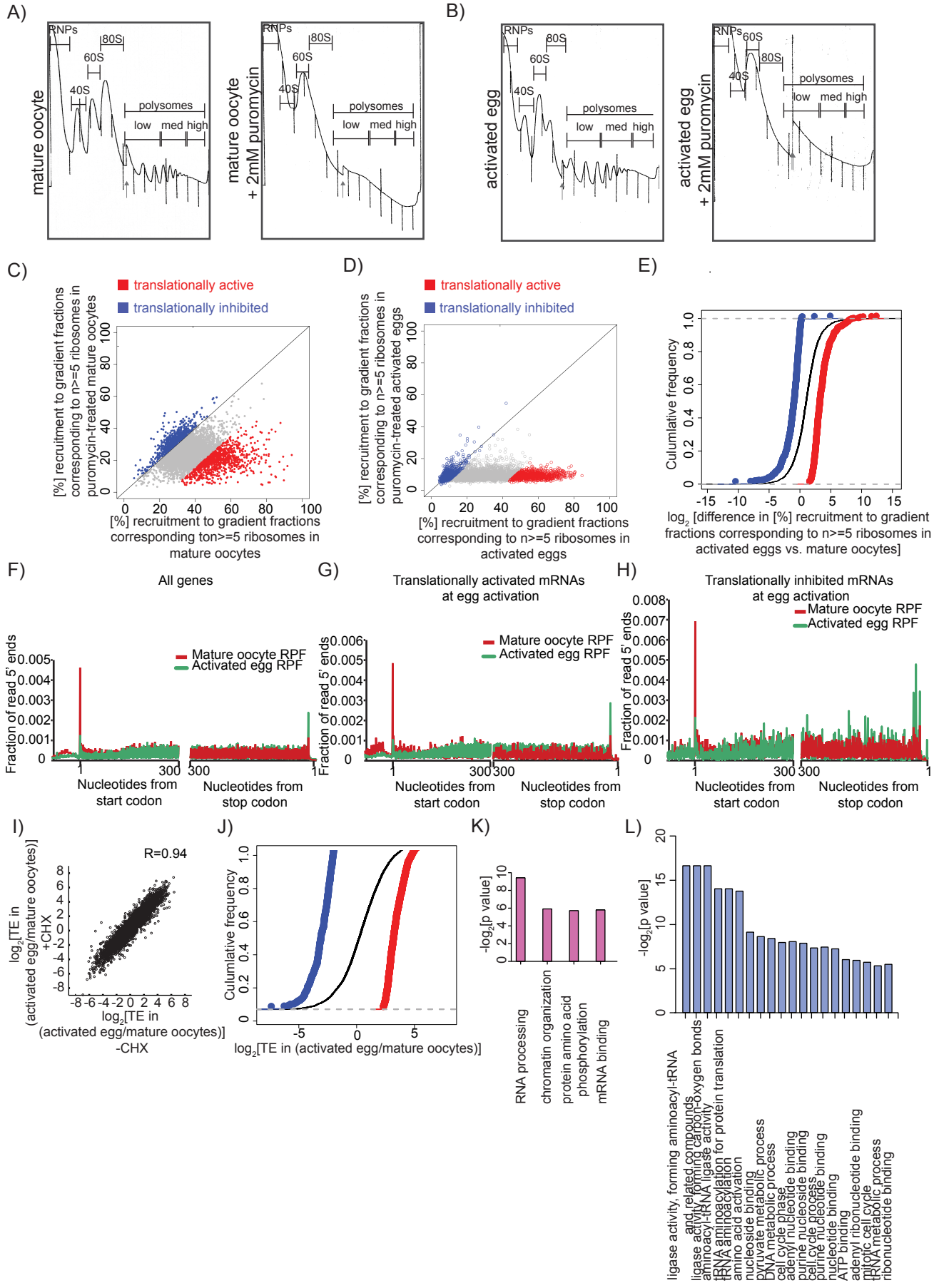
A)
mature oocyte
mature oocyte + 2mM puromycin
RNPs
40S
60S
80S
polysomes
low med high
B)
activated egg
activated egg + 2mM puromycin
C)
translationally active
translationally inhibited
[%] recruitment to gradient fractions corresponding to n>=5 ribosomes in puromycin-treated mature oocytes
[%] recruitment to gradient fractions corresponding ton>=5 ribosomes in mature oocytes
D)
[%] recruitment to gradient fractions corresponding to n>=5 ribosomes in puromycin-treated activated eggs
[%] recruitment to gradient fractions corresponding to n>=5 ribosomes in activated eggs
E)
Culumlative frequency
log2 [difference in [%] recruitment to gradient fractions corresponding to n>=5 ribosomes in activated eggs vs. mature oocytes]
F)
All genes
G)
Translationally activated mRNAs at egg activation
H)
Translationally inhibited mRNAs at egg activation
Mature oocyte RPF
Activated egg RPF
Fraction of read 5' ends
Nucleotides from start codon
Nucleotides from stop codon
I)
R=0.94
log2[TE in (activated egg/mature oocytes)] +CHX
log2[TE in (activated egg/mature oocytes)] -CHX
J)
Culumlative frequency
log2[TE in (activated egg/mature oocytes)]
K)
-log2[p value]
RNA processing
chromatin organization
protein amino acid phosphorylation
mRNA binding
L)
-log2[p value]
ligase activity, forming aminoacyl-tRNA and related compounds
ligase activity, forming carbon-oxygen bonds
aminoacyl-tRNA ligase activity
tRNA aminoacylation for protein translation
tRNA aminoacylation
amino acid activation
nucleoside binding
pyruvate metabolic process
DNA metabolic process
cell cycle phase
adenyl nucleotide binding
purine nucleoside binding
cell cycle process
purine nucleotide binding
nucleotide binding
ATP binding
adenyl ribonucleotide binding
mitotic cell cycle
tRNA metabolic process
ribonucleotide binding

Figure S3.

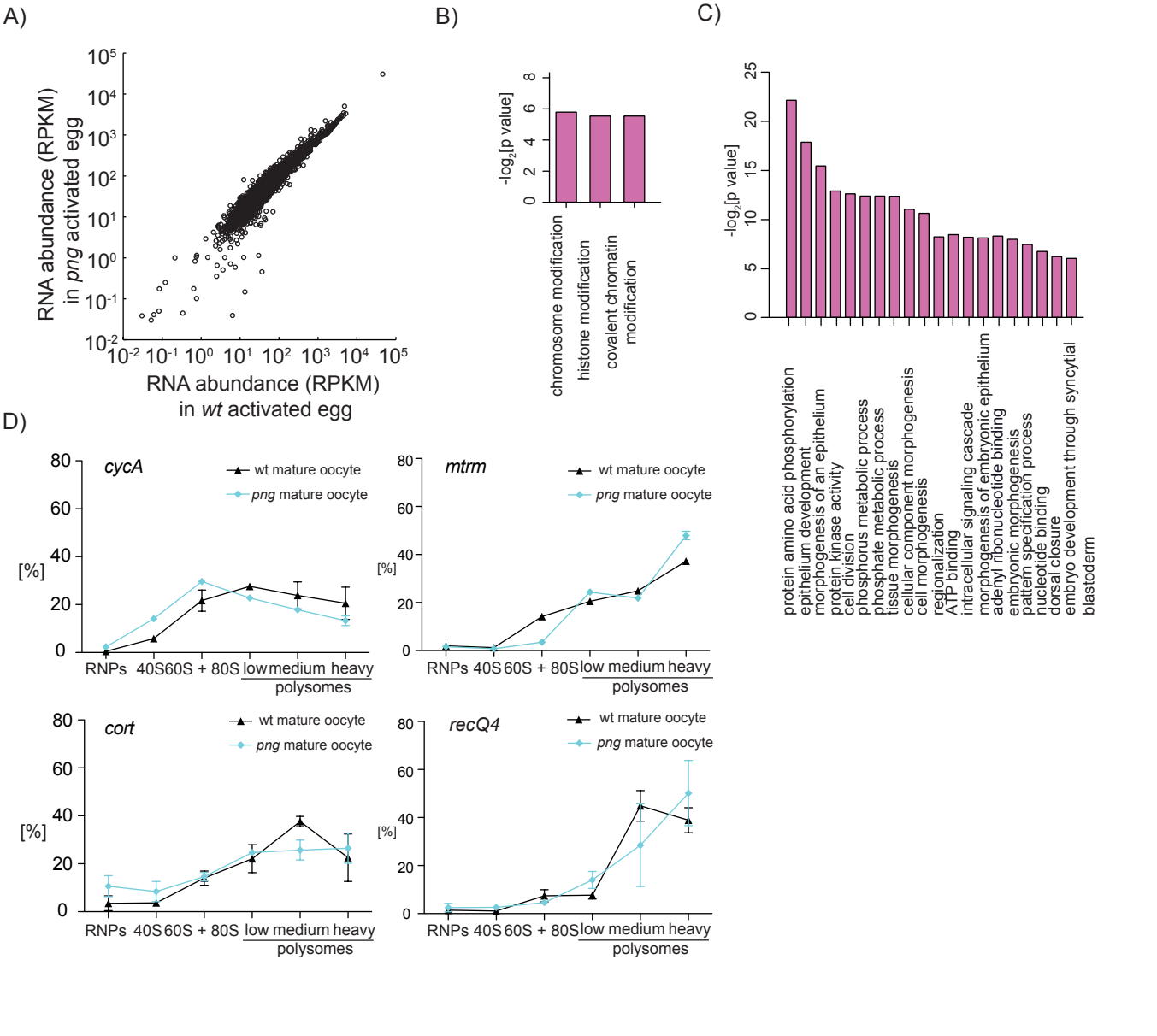
A)
RNA abundance (RPKM) in *png* activated egg
RNA abundance (RPKM) in *wt* activated egg
B)
-log2[p value]
chromosome modification
histone modification
covalent chromatin modification
C)
-log2[p value]
protein amino acid phosphorylation
epithelium development
morphogenesis of an epithelium
protein kinase activity
cell division
phosphorus metabolic process
phosphate metabolic process
tissue morphogenesis
cellular component morphogenesis
cell morphogenesis
regionalization
ATP binding
intracellular signaling cascade
morphogenesis of embryonic epithelium
adenyl ribonucleotide binding
embryonic morphogenesis
pattern specification process
nucleotide binding
dorsal closure
embryo development through syncytial blastoderm
D)
cycA
mtrm
cort
recQ4
wt mature oocyte
png mature oocyte
[%]
RNPs 40S 60S + 80S low medium heavy polysomes

Figure S4.

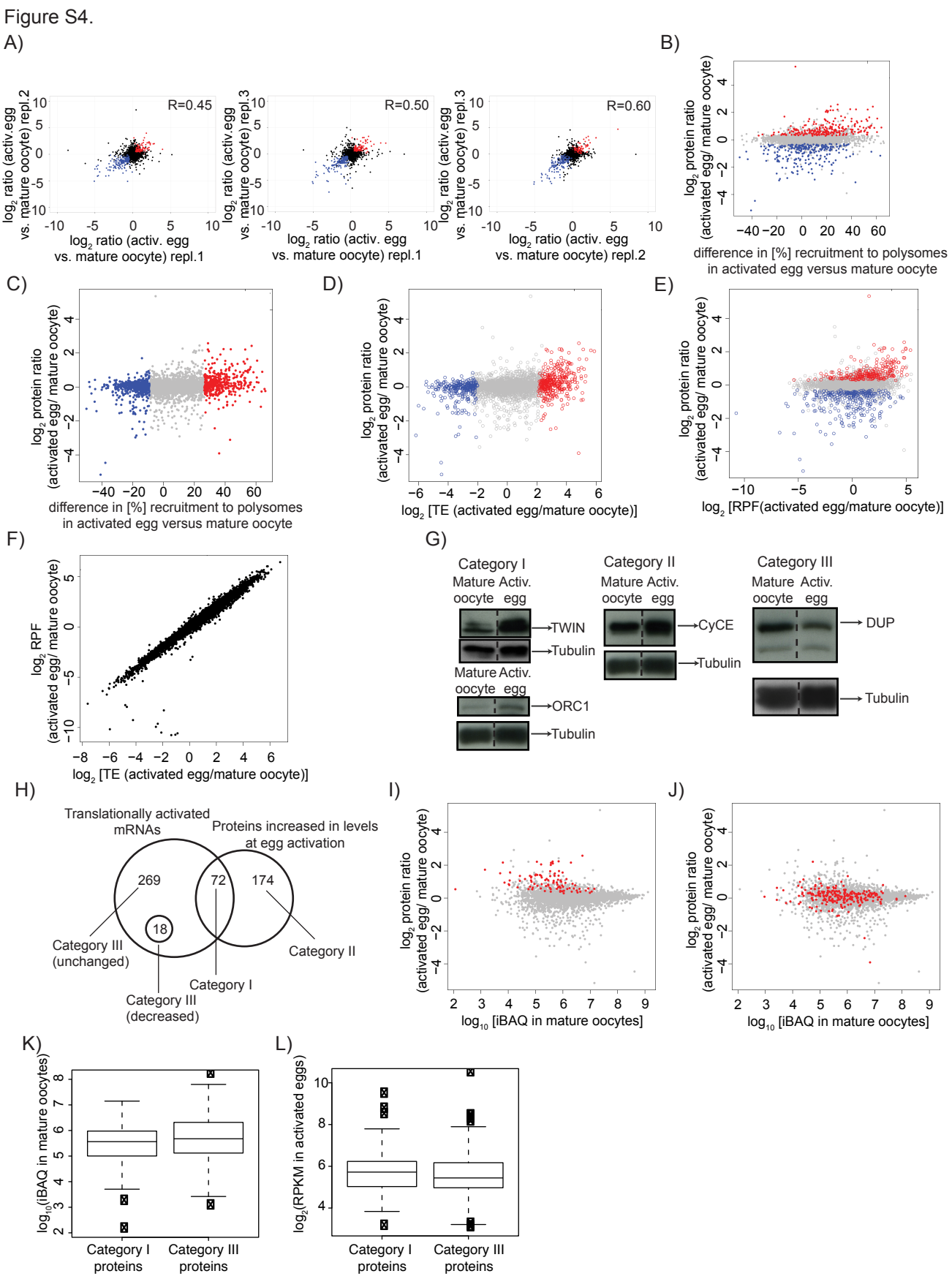
A)
R=0.45
R=0.50
R=0.60
log2 ratio (activ.egg vs. mature oocyte) repl.2
log2 ratio (activ.egg vs. mature oocyte) repl.3
log2 ratio (activ. egg vs. mature oocyte) repl.1
log2 ratio (activ. egg vs. mature oocyte) repl.2
B)
log2 protein ratio (activated egg/ mature oocyte)
difference in [%] recruitment to polysomes in activated egg versus mature oocyte
C)
D)
log2 [TE (activated egg/mature oocyte)]
E)
log2 [RPF(activated egg/mature oocyte)]
F)
log2 RPF (activated egg/ mature oocyte)
G)
Category I
Mature oocyte
Activ. egg
TWIN
Tubulin
ORC1
Category II
CyCE
Category III
DUP
H)
Translationally activated mRNAs
Proteins increased in levels at egg activation
269
72
174
18
Category III (unchanged)
Category I
Category II
Category III (decreased)
I)
log10 [iBAQ in mature oocytes]
J)
K)
log10(iBAQ in mature oocytes)
Category I proteins
Category III proteins
L)
log2(RPKM in activated eggs)

Figure S5.

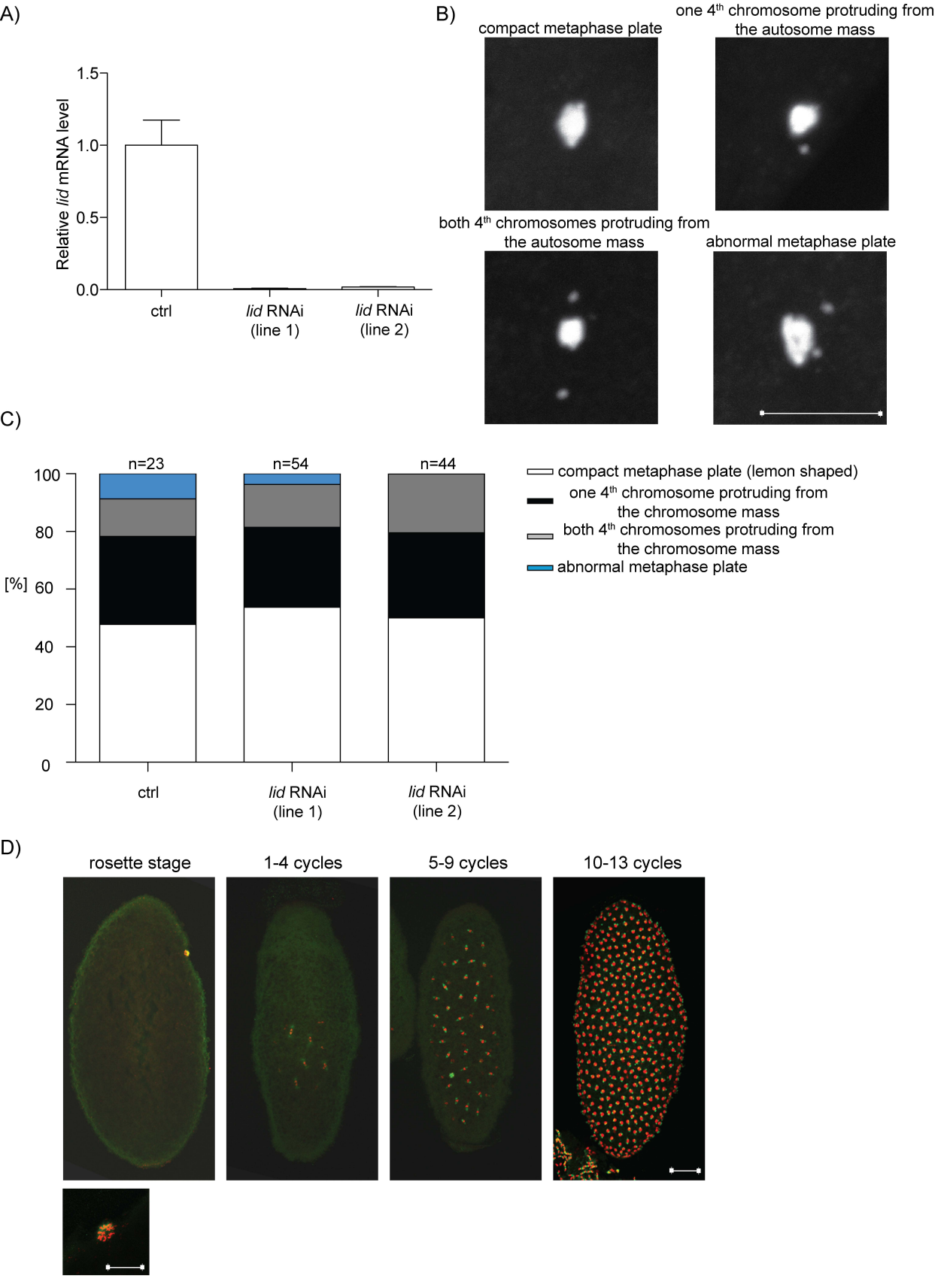
A)
Relative lid mRNA level
1.5
1.0
0.5
0.0
ctrl
lid RNAi (line 1)
lid RNAi (line 2)
B)
compact metaphase plate
one 4th chromosome protruding from the autosome mass
both 4th chromosomes protruding from the autosome mass
abnormal metaphase plate
C)
n=23
n=54
n=44
100
80
[%] 60
40
20
0
ctrl
lid RNAi (line 1)
lid RNAi (line 2)
compact metaphase plate (lemon shaped)
one 4th chromosome protruding from the chromosome mass
both 4th chromosomes protruding from the chromosome mass
abnormal metaphase plate
D)
rosette stage
1-4 cycles
5-9 cycles
10-13 cycles

Figure S6.

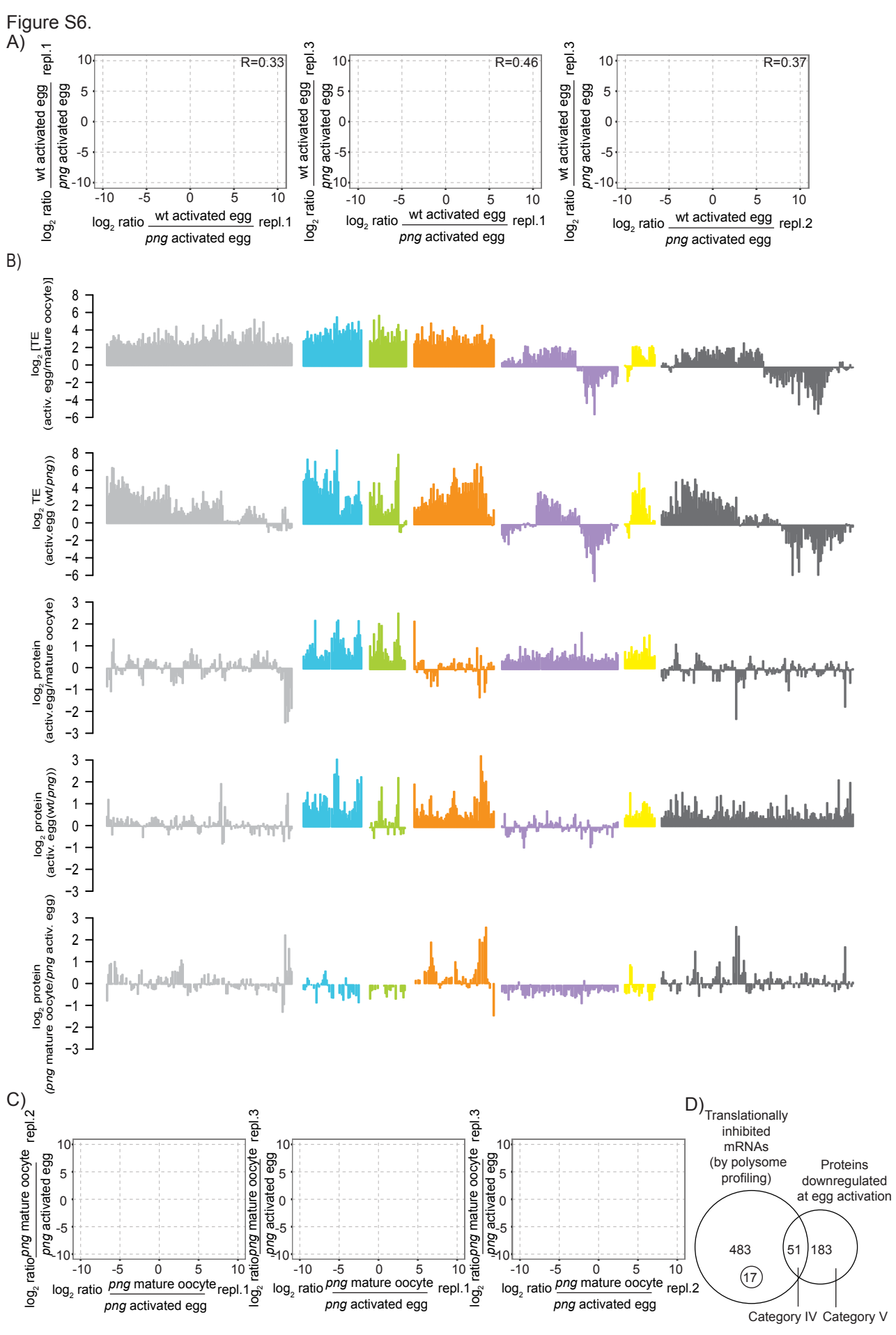
A)
R=0.33
R=0.46
R=0.37
log2 ratio wt activated egg / png activated egg repl.1
log2 ratio wt activated egg / png activated egg repl.3
log2 ratio wt activated egg / png activated egg repl.2
B)
log2 [TE (activ. egg/mature oocyte)]
log2 TE (activ.egg (wt/png))
log2 protein (activ.egg/mature oocyte)
log2 protein (activ. egg(wt/png))
log2 protein (png mature oocyte/png activ. egg)
C)
log2 ratio png mature oocyte / png activated egg repl.2
log2 ratio png mature oocyte / png activated egg repl.3
log2 ratio png mature oocyte / png activated egg repl.1
D)
Translationally inhibited mRNAs (by polysome profiling)
Proteins downregulated at egg activation
483
51
183
17
Category IV
Category V

Supplemental Figure Legends

Supplemental Figure 1. (Related to Figure 1). Transcriptional and translational profiling of mature oocytes and activated eggs.

A) Scatterplot showing on a logarithmic scale the correlation between rpkm values for: biological replicates of unfractionated inputs of mature oocytes (left panel), activated eggs (middle panel), or average rpkm (reads per kilobase per million) values of two replicate experiments of mature oocytes versus activated eggs (right panel). An rpkm of at least 4 (in the heavy polysome fraction) was used as an expression cut-off for both the mature oocyte and activated egg samples. The Pearson R^2 value is shown on each graph.

B) Same as in panel A, with the exception that the scatterplots show the rpkm correlations for two biological replicates of the mRNA sequencing data of the six polysome sucrose gradient fractions isolated from mature oocytes: RNPs, 40S, 60S+80S, low polysomes (2-4 polysomes), medium polysomes (5-9 polysomes) and heavy polysomes (10 and higher). The Pearson R^2 value is shown on each graph.

C) Same as in panel B, with the exception that the scatterplots show the rpkm correlations for two biological replicates of the six polysome sucrose gradient fractions from activated eggs.

Supplemental Figure 2. (Related to Figure 1). Polysome-profiling and ribosome footprinting analysis at egg activation

A) A representative profile of 254nm absorbance for lysates of control (left panel) and 2mM puromycin-treated lysates of wild-type mature oocytes (right panel). These polysome profiles were obtained using Brandel gradient station (Brandel), while those shown in Figures 1B and 2A were obtained using BioComp gradient station (BioComp Instruments). Gradient fractions of interest are labeled as in Figure 1B. Vertical lines mark when gradient fraction collector moved from one fraction to another. Grey arrows point to the manually controlled increase in the sensitivity setting of the absorbance reader (from 1 to 0.5). Although based on the absorbance profile the polysomes appear completely dissociated by the puromycin treatment, it is possible that some polysomes remain.

B) Same as in panel A, except 254nm absorbance profiles are shown for control (left panel) and 2mM puromycin-treated lysates of activated eggs (right panel).

C) Scatterplot showing the association of 5829 mRNAs (as a percentage of total abundance) within the sucrose gradient region that corresponds to n≥5 ribosomes after fractionation of control or puromycin-treated lysates of mature oocytes. Translationally active mRNAs (red, n=881 mRNAs) have at least 24.8% higher recruitment to the region of the gradient occupied by n≥5 ribosomes in control than in puromycin-treated mature oocytes (1SD above the median for the difference of all 5829 identified mRNAs that are above the filtering cutoff, see Extended Experimental Procedures). Translationally inhibited mRNAs (blue, n=754 mRNAs) show at least 0.8% lower recruitment to the region of the gradient occupied by n≥5 ribosomes in the absence than in the presence of puromycin. The recruitment to

polysomes in control mature oocytes is an average of two experiments, whereas the sequencing of mRNAs isolated from sucrose gradient fractions of puromycin-treated mature oocytes was only preformed once.

D) Same as panel C, except control and puromycin-treated lysates of activated eggs are presented. 953 translationally active mRNAs have by 37.6%, and 930 translationally inhibited mRNAs by 3.9%, higher recruitment to the two bottom gradient fractions in the absence than in the presence of puromycin; total n of mRNAs presented=5487.

E) Cumulative distributions of difference in polysomal recruitment after egg activation. Data were corrected for the presence of mRNAs in the same regions of the gradient after fractionation of puromycin-treated samples (See Extended Experimental Procedure for details). The same cut-offs are applied and the categories are the same as in Figure 1C. 729 mRNAs are translationally repressed mRNAs (blue), 3557 translationally unchanged (black) and 802 are translationally activated (red).

F) Fraction of RPFs near the ends of ORFs for all genes. The fraction of RPF 5´terminal to a given position relative to the rest of the ORF is computed for each mRNA in mature oocyte or activated egg samples not treated with cycloheximide, and the average fraction across all quantified mRNAs with an ORF ≥600 nts is plotted. RPFs are shifted +15 nucleotides to account for the offset between the RPF 5' terminus and the first nucleotide in the ribosome A site.

G) As in E), but for the subset of mRNAs shown in Figure 1D for which TE increased during the transition from mature oocyte to activated egg.

H) As in E), but for the subset of mRNAs shown in Figure 1D for which TE decreased during the transition from mature oocyte to activated egg.

I) Reproducibility of translational efficiency fold change. The ratio (log_2) of activated egg translational efficiency to mature oocytes translational efficiency for samples in which cycloheximide was excluded (-CHX) was plotted against that for the samples treated with cycloheximide (+CHX), showing all quantified genes (n=5824; Spearman *R* = 0.94).

J) Cumulative distributions of changes in translational efficiency after egg activation. The same cut-offs are applied and the categories are the same as in Figure 1D. 986 mRNAs are translationally repressed mRNAs (blue), 4408 translationally unchanged (black) and 448 are translationally activated (red).

K) Gene Ontology (GO) term categories for 301 mRNAs that are translationally activated at egg activation according to both ribosome footprinting and polysome profiling. The four GO categories with FDR p-value <0.05 are shown.

L) Same as K) except shown are the top 20 GO categories for 213 mRNAs that are translationally inhibited at egg activation according to both ribosome footprinting and polysome profiling. All GO categories have FDR p-value <0.05.

Supplemental Figure 3. (Related to Figure 2). GO-term analysis of mRNAs based on the PNG-dependence of mRNA's translational status at egg activation

A) Scatterplot showing the correlation between average rpkm (reads per kilobase per million) values of two replicate experiments of wild-type versus *png* activated eggs.

B), C) Top 20 Gene Ontology (GO) term categories for mRNAs translationally activated at egg activation that are B) PNG-independent or C) PNG-dependent. FDR p-value is shown.

D) Quantitative RT-PCR analysis of *cycA*, *mtrm*, *cort* and *recQ4* mRNA abundance in polysome gradient fractions in control mature oocytes (black) as compared to *png* mature oocytes (turquoise) shows that PNG does not influence the translational status of these mRNAs prior to egg activation. mRNA abundance in each fraction is presented as a percentage of total in all fractions of one sample (n=1 experiment). Error bars indicate SD within triplicate reactions of a single qRT-PCR experiment.

Supplemental Figure 4. (Related to Figure 3). Quantitative mass spectrometry analysis at egg activation: correlation among replicates and overlap with translatome measurements

A) Scatterplots showing the correlation between the $\log_2$ of normalized protein ratios for three biological replicates of experiments comparing protein levels in mature oocytes and activated eggs. Limma analysis (see Extended Experimental Procedures) was used to define proteins significantly upregulated (red) and downregulated (blue) at egg activation. Proteins whose normalized ratio averaged between three

replicates had a *p*-value lower than 0.05 were considered as significantly changed. Pearson correlation is displayed on each panel.

B) A scatterplot showing the relationship between $\log_2$ of protein ratios at egg activation and the difference in polysomal recruitment ($n \geq 5$ ribosomes) for mRNAs that encode for them. In red, proteins significantly increased at egg activation are shown, whereas blue represents those significantly decreased.

C) Same as in B) except that mRNAs translationally upregulated according to polysome profiling at egg activation are shown in red whereas blue represents translationally inhibited mRNAs. The cutoff is described in Figure 1C.

D) Same as Figure 3A) except mRNAs defined as significantly translationally upregulated according to ribosome footprinting are marked in red, whereas translationally inhibited mRNAs are shown in blue. Only factors identified by both approaches are represented.

E) Same as Figure 3A), except the change in RPF (ribosome protected fragment; measured in rpkm) at egg activation is shown instead of the change in translational efficiency. Only factors identified by both approaches are represented.

F) Scatterplot showing a relationship between $\log_2$ of change in translational efficiency and change in RPF at egg activation.

G) Western blot validation of candidates belonging to Category I (Twin and ORC1); Category II (CycE; reprobed on the same membrane as ORC1) and Category III (DUP; reprobed on the same membrane as GNU in Figure 6B).

H) Same as Figure 3D, only translationally activated mRNAs are identified according to polysome profiling. Only factors identified by both approaches are represented.

I) Scatterplot showing the relationship between the $\log_2$ of change in protein levels at egg activation and $\log_{10}$ of protein abundance in mature oocytes for Category I proteins in Figure 3D.

J) Same as I) except only Category III proteins from Figure 3D are represented.

K) Boxplot showing $\log_{10}$ of protein abundance in mature oocytes for Category I and Category III proteins from Figure 3D. Boxplot features are the same as in Figure 2C.

L) Same as K) except the $\log_2$ of mRNA abundance (rpkm) in activated eggs is shown.

Supplemental Figure 5. (Related to Figure 4). Lid knockdown is efficient in TRiP RNAi lines, and Lid is not required for metaphase arrest in mature oocytes

A) qRT-PCR analysis of *lid* mRNA levels in mature oocytes dissected from females with only the maternal-tubulin-Gal4 driver (control) or females with one of either of the two *lid* RNAi lines and the maternal-tubulin-Gal4 driver. *lid* RNAi line 1 is BL35706, and *lid* RNAi line 2 is BL36652. *lid* mRNA levels are very efficiently decreased in maternal-tubulin-Gal4 driven *lid* RNAi lines relative to the control (*lid* levels in the control are set to 1). *Actin5c* was used for normalization. Error bars indicate the range of expression levels measured (minimum and maximum) for triplicate

reactions performed within one representative qRT-PCR experiment.

B) Representative images of different configurations of the DAPI-stained metaphase I plate in control mature oocytes. Scale bar, 10 μm.

C) Quantification of categories shown in panel B in mature oocytes dissected from control females or females with germ-line knockdown of *lid* (n=1 experiment). n=number of oocytes scored.

D) Representative images of different stages within the first two hours of embryonic development in wild-type embryos: completed meiosis, with meiotic products in a rosette (image below shows an enlargement of a rosette; scale bar, 20 μm), embryos that went through 1-4 nuclear divisions, or 5-9 divisions or 10-13 divisions (entered syncytial blastoderm). DNA is shown in red and tubulin in green. Scale bar, 50 μm.

Supplemental Figure 6. (Related to Figures 5 and 6). Proteome remodeling at egg activation in *png* mutants

A) Same as in Figure S4A except that the scatterplot shows the correlation among the $\log_2$ of normalized protein ratios for three biological replicates of experiments comparing protein levels in wild-type and *png* activated eggs. Proteins that according to Limma have significantly higher levels in wild-type than *png* activated eggs are shown in red, whereas those with significantly lower levels in wild-type versus *png* activated eggs are displayed in blue.

B) For the categories shown in Figure 5A), this figure shows from top to bottom: $\log_2$ change in translational efficiency between activated eggs and mature oocytes; $\log_2$ change in translational efficiency between activated

eggs in wild-type versus *png* mutant; normalized $\log_2$ ratios of protein levels in wild-type activated eggs versus mature oocytes; normalized $\log_2$ ratios of protein levels in wild-type versus *png* mutant activated eggs; or normalized $\log_2$ ratios of protein levels in *png* mutant mature oocytes versus activated eggs. Segments of the figure are colored in the same way as the category from Figure 5A they represent.

C) Same as in Figure S4A except that the scatterplots show the correlation among the $\log_2$ of normalized protein ratios for three biological replicates of experiments comparing protein levels in *png* mature oocytes and activated eggs. Proteins that according to Limma have significantly higher levels in *png* mature oocytes than *png* activated eggs are shown in blue and those with significantly lower levels in *png* mature oocytes as compared to *png* activated eggs are displayed in red.

D) Same as Figure 6A, with the exception that polysome profiling was used to define the translatome. The criteria for characterizing mRNAs as translationally activated or inhibited at egg activation is described in Figure 1C and Extended Experimental Procedures. Only factors identified by both approaches are represented.

Supplemental Tables

Table S1 (Related to Figure 1). Polysomal profiling data for all mRNAs in: lysates of mature oocytes (two independent biological replicates are shown separately), puromycin-treated lysates of mature oocytes, lysates of activated eggs (two independent biological replicates are shown

separately) and puromycin-treated lysates of activated eggs. Only mRNAs that pass the significance cutoff for expression are shown (see Supplemental Experimental Procedures). Shown are: normalized rpkm (rpkm normalized according to spiked-in *S. cerevisiae* mRNA, see Extended Experimental Procedures) and percentage (of total) abundance within each of the six polysomal gradient fractions of interest.

Table S2 (Related to Figure 2). Ribosome footprinting data for all detected mRNAs. Presented are: mRNA abundance in rpkm ('RNA' columns), ribosome protected fragments in rpkm ('RPF' columns) and translational efficiency ('TE' columns) for mature oocytes, as well as wild-type (wt) and *png* activated eggs. A separate Excel sheet named "png_mature_oocyte_withCHX" contains this information for *png* mature oocytes.

Table S3 (Related to Figures 3, 5 and 6). Identification and quantification data for all identified protein in sample pair comparing protein abundance in: wild-type activated eggs versus wild-type mature oocytes (Sheet "wt (activ_egg.vs.mature_oocyte)"), wild-type activated eggs versus *png* activated eggs (Sheet "wt_activ_egg.vs.png_activ_egg"), and *png* mature oocytes versus *png* activated eggs (Sheet "png(mature_oocyte.vs.act_egg)"). The proteins statistically increased in levels according to Limma are shown in red, whereas those decreased are shown in blue. The proteins are merged according to "Protein Descriptions" and some appear in more than one row.

Table S4 (Related to Figures 3,5 and 6). List of: translationally regulated mRNAs (and their dependence on PNG); proteins whose levels change at egg activation in wt and *png* mutant background as well as in wt activated eggs versus *png* activated eggs; proteins from Categories I-V in Figures 3 and 6; proteins belonging to color coded Venn diagram segments in Figures 5 and 6.

Supplemental Discussion

Our identification of translationally regulated mRNAs opens the path to define the mRNA features and mechanisms responsible for translational control. This is likely to be complex. Work on *Tl*, an mRNA translationally upregulated at the onset of embryogenesis, suggests that secondary structure and/or multiple motifs control its translational status in early embryos (Coll et al., 2010). Consistent with this, we did not identify a unique sequence motif by bioinformatics analysis of either 5' UTRs and 3' UTRs of mRNAs that are translationally upregulated at egg activation (data not shown). Sequence motifs identified by these analyses were not compelling as they were rather degenerate. 3' UTR and 5' UTR motif analyses of translationally downregulated mRNAs also did not yield a particular motif.

Supplemental Experimental Procedures

Drosophila stocks

All flies were kept at 18, 22 or 25°C according to standard procedure (Greenspan, 1997). *Oregon R* flies were used as a wild-type control. The null png^{1058} allele was previously described (Fenger et al., 2000; Shamanski and Orr-Weaver, 1991) as well as the mr^{1} and mr^{2} alleles (Kashevsky et al., 2002; Reed and Orr-Weaver, 1997). Unfertilized eggs were collected from crosses to $twine^{HB5}$ mutant males, which fail to make sperm (Courtot et al., 1992). The two *lid* RNAi lines from the Transgenic RNAi project (TRiP), one in the Valium 21 vector (BL35706) and the other in Valium 22 (BL36652), were obtained from the Bloomington Drosophila Stock Center. The maternal-tubulin-Gal4 P{matα4-GAL-VP16}V37 driver also was from the Bloomington Stock Center.

Mature oocyte isolation and collection of activated eggs

To facilitate isolation of stage 14 mature oocytes, dissected ovaries were treated with 5 mg/ml of collagenase in Grace's media and incubated for 10 min on a nutator at room temperature (RT). Activated eggs were collected at RT every 2 hours and stored at 4°C for up to 10 hours or until sufficient numbers were collected. The pooled eggs were dechorionated in 50% bleach for 5 minutes, extensively washed in water and transferred into an Eppendorf tube for lysis (either for quantitative mass spectrometry, Western blots or polysome profiling).

Sample preparation for quantitative mass spectrometry

For quantitative mass spectrometry, samples were lysed in SDT lysis buffer (4% w/v SDS, 100mM Tris-HCl pH 7.6 and 0.1M DTT) and incubated for 5 minutes at 95°C. After sonication, lysates were centrifuged at 13000 rpm for 5 minutes, and the supernatants were flash frozen. Due to the large amount of SDS and DTT in SDT buffer, these lysates were incompatible with colorimetric assays to determine protein concentration. Therefore, the protein concentration in each sample was estimated by running it on SDS-PAGE gel together with a lysate of known protein concentration (estimated by Bradford assay, BioRad), followed by staining with GelCode Blue Stain Reagent (Pierce), scanning, and ImageJ quantitation.

Digestion of the proteins was performed according to a previously published FASP (filter-aided sample preparation) protocol (Wisniewski et al., 2009). Following elution from filter units, digested peptides were acidified with 10 % trifluoracetic acid and subjected to stable isotope labeling (peptide dimethylation) using Sep-Pak® cartridges (Vac 1cc (50 mg) tC_{18}, Waters) (Boersema et al., 2009). If in one biological replicate one sample within the sample pair was labeled with “light” reagent (formaldehyde-H2 and sodium cyanoborohydride) in the next replicate it would be labeled with “heavy” reagent (formaldehyde-D2 and sodium cyanoborohydride). For the third replicate the labeling would be swapped again.

The labeled samples within one biological replicate were combined and dried down using the speed vacuum centrifuge. The peptides were reconstituted in IPG strip rehydration solution and separated by isoelectric

focusing using an Agilent 3100 OFFGEL Fractionator. The standard OFFGEL kit protocol was applied in combination with ImmobilineTM DryStrips (ph 3-10 NL, 13 cm, GE Healthcare). Afterwards, 12 peptides fractions were collected and desalted using Thermo Scientific Aspire RP30 Desalting Pipette Tips. The peptide samples were dried in speed vacuum centrifuge and dissolved in 0.1 % formic acid prior to liquid chromatography-mass spectrometry analysis.

LC-MS/MS

Peptides were separated using the nanoAcquity UPLC system (Waters) fitted with a trapping (nanoAcquity Symmetry C18, 5µm, 180 µm x 20 mm) and an analytical column (nanoAcquity BEH C18, 1.7µm, 75µm x 200mm). The outlet of the analytical column was coupled directly to an LTQ Orbitrap Velos (Thermo Fisher Scientific) using the Proxeon nanospray source. Solvent A consisted of 0.1 % formic acid in water and solvent B 0.1 % formic acid in acetonitrile. The samples (5 µL) were loaded with a constant flow of solvent A at 15 µL/min onto the trapping column. Trapping time was 1 minute. Peptides were eluted via the analytical column at a constant flow of 0.3µL/min. During the elution step, the percentage of solvent B increased in a linear fashion from 3% to 7% in 10 minutes, followed by an increase to 25% in 110 min and to 40% in 10 min.

The peptides were introduced into the mass spectrometer via a Pico-Tip Emitter (360 µm OD x 20 µm ID; 10 µm tip New Objective), applying a spray voltage of 2.1 kV and a capillary temperature of 300 °C. Full scan MS spectra with mass range 300-1700 m/z were acquired in

profile mode in the Orbitrap with a resolution of 30000. The ion accumulation time was set at a maximum of 500 ms with a limitation of 10^6 ions. The 15 most intense ions exceeding 1000 counts were subjected to collision-induced dissociation in the LTQ. A normalized collision energy of 40 % was used, and the fragmentation was performed after accumulation of 3 x 10^4 ions or after a filling time of 50 ms for each precursor ion (whichever occurred first). MS/MS data were acquired in centroid mode. Charge state screening was enabled, and only doubly and triply charged precursor ions were selected for MS/MS. The dynamic exclusion list was restricted to 500 entries with a maximum retention period of 30 s and a relative mass window of 7 ppm. For internal mass calibration, a lock mass correction using a background ion (m/z 445.12003) was applied.

Quantitative mass spectrometry data analysis

The mass spectrometric raw data of each replicate was separately processed using MaxQuant (version 1.1.1.25) (Cox and Mann, 2008) and MS/MS spectra were searched using the Andromeda search engine (Cox et al., 2011) against a Uniprot species specific (*Drosophila melanogaster*; 16519 entries) database. Enzyme specificity was set to trypsin/P, and a maximum of two missed cleavages were allowed. Cysteine carbamidomethylation was used as a fixed modification, whereas methionine oxidation and protein N-terminal acetylation were used as variable modifications. The minimum peptide length was set to six amino acids. The initial maximum allowed mass tolerance was set to 20 ppm for peptide masses, followed by 6 ppm in the main search and 0.5 Da for fragment ion masses. False discovery rates for peptide and protein

identification were set to 1 %. At least one unique peptide was required for protein identification. The protein identification was reported as an indistinguishable “protein group” if no unique peptide sequence to a single database entry was identified.

Statistical analysis of quantitative mass spectrometry results

As mature oocytes, unlike activated eggs, still contain some follicle cells, we removed from further analysis proteins characteristic of follicle cells (Chorion proteins (Cp), Follicle cell proteins (Fcp), vitellogenins and yellow-g and yellow-g2, dec1, CG13084, CG31928, CG4009) and some potential follicle cell proteins (CG10623, CG1077, CG11381, CG32642, CG34333) as well as Oat, Obp19C, CG10623, CG14624, CG14309, CG14834, CG34417, CG5958, CG6579 and CG9336. In the case of comparing proteomes of wild-type and *png* activated eggs, several additional potential follicle cell proteins were removed from further analysis: CG10777, mal, Femcoat and Yl.

We show normalized H/L ratios from the three biological replicates of each tested sample pair in Supplementary Table 3. The average normalized ratio was calculated and used for further analysis only for the proteins with ratios quantified in at least two of the three replicates. Because we alternated between biological replicates which sample within a sample pair was labeled as “light (L)”, or “heavy (H)”, the signs of the normalized ratios also had to be adjusted accordingly (i.e. their sign flipped). In the case of sample pairs comparing protein levels in wild-type at egg activation, we had two technical replicates of the first biological replicate. For this, we first merged those two technical replicates by gene

symbol, and we then calculated the average of the normalized H/L ratio. If the protein ratio was quantified in only one of the technical replicates, it was nevertheless considered.

The statistical analysis of the mass spectrometric data was performed using the Limma package in R/Bioconductor (Gentleman et al., 2004). After fitting a linear model to the data, an empirical Bayes moderated t-test was used and *p*-values were reported. The *p*-value of the average normalized ratio (calculated from three biological replicates) for significantly changed proteins is lower than 0.05. Correlations between replicates were calculated in R using Pearson correlation.

The iBAQ algorithm was used for estimation of the abundance of different proteins within a single sample (proteome) (Schwanhausser et al., 2011). It normalizes the summed peptide intensities against the number of the theoretical observable peptides of the protein.

Western Blots, and Antibody dilutions used for Western Blots as well as immunofluorescence

The following dilutions of the primary antibodies were used: rat anti-tubulin (yol1/34 and yl1/2, 1:500) [Novus Biologicals], rabbit anti-Scra (1:1000) (Goldbach et al., 2010), rat anti-Dco (1:1000) (Preuss et al., 2004), guinea pig anti-GNU (1:5000) (Lee et al., 2003), guinea pig anti-Mtrm (1:1000) (Xiang et al., 2007), rabbit anti-Orc1 (1:1000) (Asano and Wharton, 1999), guinea pig anti-Cyclin E (1:7000) (Ivanovska et al., 2005), rabbit anti-Hsf (1:2000)(Westwood et al., 1991), guinea pig anti-Dup (1:1000) (Whittaker et al., 2000), rat anti-Rm62 (1:200) (Boeke et al., 2011), rabbit anti-Twin (1:1000) (Temme et al., 2004), and anti-Armadillo (1:500) (Developmental

Studies Hybridoma Bank). For secondary antibodies we used HRP-conjugated secondary antibodies (anti-rat 1:5000 dilution, anti-guinea pig 1:10000 dilution, anti-rabbit at 1:10000 dilution and anti-mouse at 1:3000 dilution) (Jackson ImmunoResearch). For detection, membranes were incubated with the Pierce ECL 2 Western Blotting Substrate (Thermo Scientific) system for 1 minute.

To reprobe membranes with another antibody following detection, we rinsed the membrane in Phosphate Buffer Saline (PBS) + 0.05% Tween and then incubated it for 30 minutes in Restore Plus Western Blot Stripping Buffer (Thermo Fisher Scientific). Finally, we washed the membrane three times for 10 minutes in PBS + 0.05% Tween, blocked it in 5% milk in PBS and proceeded with the primary antibody incubation.

Fixed embryos were stained with monoclonal anti-alpha tubulin [clone DM1A] (1:250) (Sigma Aldrich) followed by Alexa 488-conjugated anti-mouse antibody (1:1000) (Invitrogen) to visualize microtubules, and propidium iodide to visualize DNA.

Immunofluorescence of egg chambers

Mature oocytes were fixed and stained with DAPI as described, with the exception that the fixation was done in 4% formaldehyde (Ivanovska et al., 2004).

Polysome Analysis

For polysome profiling, collected mature oocytes and activated eggs (see sample collection section) were lysed in a buffer containing 0.25 M KCl, 0.05 M Tris-HCl (pH 7.3), 0.05 M MgCl, 0.2% Triton X-100, 400U/ml of extract of RNasin (Promega), 2.5 mg/ml heparin, and 0.5 mg/ml

cycloheximide (Mermod and Crippa, 1978). The lysates were cleared by centrifugation at 10000 rpm for 5 minutes, flash frozen in liquid nitrogen and stored at -80°C. The frozen lysates were pooled together, and 60 μg of total RNA was used to isolate RNA from unfractionated inputs, while 540 μg of total RNA was applied to 11 ml of a 10-50% linear sucrose gradient prepared in 0.25 M KCl, 0.05 M Tris-HCl (pH 7.3), 0.025 M MgCl and 0.5 mg/ml cycloheximide. The gradients were centrifuged in a Beckman SW-41Ti rotor at 36000 rpm for 2 hours at 4°C. Samples were fractionated by upward displacement with 60% sucrose on a gradient fractionator (Brandel). The absorbance measurement at 254 nm was performed using an ISCO UA-5 monitor. The fractions were pooled to generate samples of RNPs, 40S, 60S + 80S, low (2-4) polysomes, medium (5-9) polysomes and heavy (10-higher) polysomes. Prior to RNA extraction, in vitro transcribed 5ng of Firefly luciferase (Promega) and 5ng of *S. cerevisae* mRNA (purified by 2 rounds of oligo-dT selection from *S. cerevisae* total RNA; kindly provided by Ines Anna Drinberg and Alexander Subtelny from the lab of David Bartel) were added to each pooled fraction to allow for normalization between the fractions during the analysis of mRNA sequencing and qRT-PCR. The exception was that for the first biological replicate preparation of the wild-type mature oocytes, yeast mRNA was added to each of the individual 14 sucrose gradient fractions rather than to the six pooled fractions of interest. For the second replicate of wild-type mature oocytes and activated eggs as well as for puromycin-treated mature oocytes, we also added in vitro transcribed fire fly luciferase to the fractions to use for normalization in qRT-PCR

experiments (luciferase was omitted in the first replicate preparation of wild-type mature oocytes and activated eggs).

Polysome to monosome ratios (P/M) were calculated by subtracting from the sum of A_{254nm} absorbance for monosomes or medium plus heavy polysomes ($n \geq 5$ ribosomes) minimal absorbance of the entire profile. Then, the portion (percentage) of the profile (with the exception of RNPs) that was occupied by $n \geq 5$ ribosomes was divided by the portion of the profile occupied by monosomes.

For solely visualization of polysomes, 60 μg of total RNA was applied to the 11 ml of 10-50% linear sucrose gradients, centrifuged as above and analyzed using the Biocomp gradient station (Biocomp).

mRNA sequencing data analysis

RNA-seq reads were checked with FastQC (http://www.bioinformatics.babraham.ac.uk/projects/fastqc/). Low quality reads and adapter sequences were removed with FASTX-Toolkit (http://hannonlab.cshl.edu/fastx_toolkit/index.html) when necessary. mRNAs associated with six different fractions of polysomal gradient (RNPs, 40S, 60S+80S, low polysomes, medium polysomes and heavy polysomes) were separated based on their barcodes. The Drosophila dm3 genome (from UCSC Genome Bioinformatics) and the *S.cerevisiae* genome (from Ensembl assembly EF2 release 62) were merged, and a new gene annotation file was created by combining fly .gtf with yeast .gtf downloaded from the same sources. Then, RNA-seq reads were mapped to the merged genome using TopHat v1.3.2 (Trapnell et al., 2009) with option --segment-length 20, and guided with the merged annotation file.

Next, htseq-count (http://www-huber.embl.de/users/anders/HTSeq/doc/overview.html) was used for counting the reads in the fly and yeast genes. Any reads that mapped to rRNAs were removed from further analysis. We represented fly and yeast mRNA levels with rpkm (reads per kilobase per million of mapped reads): rpkm = 10^9 (read count in gene exons/gene length) / (total fly reads +total yeast reads). If a gene has multiple isoforms, the length of its longest transcript was used for gene length. To compare quantitatively the levels of every mRNA across the polysome gradient fractions, we added into each fraction the same amount of *S. cerevisiae* mRNA as an exogenous spike-in. We choose *S. cerevisae* mRNA as an external standard because it is a mix of mRNAs of varying lengths and nucleotide composition, so its complexity is similar to our experimental sample. Another favorable feature is that when *S. cerevisiae* mRNA was added at ~0.5% of total RNA to Drosophila oocyte or egg sucrose gradient fractions, only ~0.003% of sequencing reads had to be discarded due to potential overlap.

For each polysome gradient fraction, we calculated the average of the top 20 highly expressed yeast genes sorted by the highest abundance in the RNP fraction. The scaling factors were derived with the assumption that all the polysome gradient fractions should have this same average gene expression level of *S.cerevisiae* genes, because the same amount of spike-in was added into each fraction from the moment the fractions were collected and fused. The fly mRNA levels were normalized with the corresponding yeast scaling factor. Only genes with rpkm greater or equal to 4 were considered expressed. When comparing different conditions, an

mRNA had to have an rpkm greater or equal to 4 in all conditions to be considered in the analysis. For each fly gene, the normalized mRNA levels of its six fractions were summed, and the percentage of the mRNA in each fraction was calculated by dividing its normalized level by this sum. The puromycin-treated samples were analyzed in the same way as the control (untreated) samples. From the percentage expression of an mRNA in the n≥5 ribosome fractions of the puromycin-untreated sample we subtracted percentage expression in the same gradient regions of the puromycin-treated sample, resulting in the estimate of the polysomal association of each mRNA.

MetaORF analysis

Ribosome profiling and RNA-seq data were used to calculate translational efficiencies for individual genes as described (Subtelny et al., 2014), except reads with 5′ ends mapping within the first 50 nt of each ORF were disregarded. TEs were considered only for genes exceeding a cutoff of 10 RPM (reads per million uniquely mapped reads) in both the RNA-seq and ribosome protected fragment libraries.

Quantitative RT-PCR

In the experiment with polysome gradient fractions, 1μl of RNA per fractions was used in a 20μl cDNA synthesis reaction that was performed according to manufacturer's instructions (Promega Reverse Transcription System), using oligo dT primers. Primer sequences are available on request. PerfeCTa SYBR Green FastMix (Quanta BioSciences) was used in quantitative PCR reactions that were performed on a 7300 Real time PCR system (Applied Biosystems).

To measure *lid* knockdown, total RNA was isolated (as described under RNA isolation) from mature oocytes dissected from females that were the progeny of the following crosses: wild-type virgin females and maternal-tubulin-Gal4 driver males (control) or virgin females of either of the two TRiP *lid* RNAi lines and maternal-tubulin-Gal4 driver males. The RNA was treated with a TURBO DNA-free kit (Ambion), and 500ng of the resulting RNA was used in a 20μl cDNA synthesis reaction that was performed according to manufacturer's instructions (Promega Reverse Transcription System), using random primers. The levels of *lid* RNA and the *actin 5C* control were quantified by qPCR (primers available on request).

Data analysis

GO analysis was performed using David Bioinformatics Resources 6.7 with BP_FAT and MP_FAT as selected GO term categories (Huang da et al., 2009).

The boxplots were created with the boxplot functions from R package.

Importantly, when comparing results obtained by different experimental approaches or comparing different samples by same methodology, we only considered data points present in both datasets.

Supplemental References

Asano, M., and Wharton, R.P. (1999). E2F mediates developmental and cell cycle regulation of ORC1 in Drosophila. The EMBO journal *18*, 2435-2448.

Boeke, J., Bag, I., Ramaiah, M.J., Vetter, I., Kremmer, E., Pal-Bhadra, M., Bhadra, U., and Imhof, A. (2011). The RNA helicase Rm62 cooperates with SU(VAR)3-9 to re-silence active transcription in Drosophila melanogaster. PLoS One *6*, e20761.
Boersema, P.J., Raijmakers, R., Lemeer, S., Mohammed, S., and Heck, A.J. (2009). Multiplex peptide stable isotope dimethyl labeling for quantitative proteomics. Nat Protoc *4*, 484-494.
Coll, O., Villalba, A., Bussotti, G., Notredame, C., and Gebauer, F. (2010). A novel, noncanonical mechanism of cytoplasmic polyadenylation operates in Drosophila embryogenesis. Genes & Dev *24*, 129-134.
Courtot, C., Fankhauser, C., Simanis, V., and Lehner, C.F. (1992). The Drosophila cdc25 homolog twine is required for meiosis. Development *116*, 405-416.
Cox, J., and Mann, M. (2008). MaxQuant enables high peptide identification rates, individualized p.p.b.-range mass accuracies and proteome-wide protein quantification. Nat Biotechnol *26*, 1367-1372.
Cox, J., Neuhauser, N., Michalski, A., Scheltema, R.A., Olsen, J.V., and Mann, M. (2011). Andromeda: a peptide search engine integrated into the MaxQuant environment. J Proteome Res *10*, 1794-1805.
Fenger, D.D., Carminati, J.L., Burney-Sigman, D.L., Kashevsky, H., Dines, J.L., Elfring, L.K., and Orr-Weaver, T.L. (2000). PAN GU: a protein kinase that inhibits S phase and promotes mitosis in early Drosophila development. Development *127*, 4763-4774.
Gentleman, R.C., Carey, V.J., Bates, D.M., Bolstad, B., Dettling, M., Dudoit, S., Ellis, B., Gautier, L., Ge, Y., Gentry, J*., et al.* (2004). Bioconductor: open software development for computational biology and bioinformatics. Genome Biol *5*, R80.
Goldbach, P., Wong, R., Beise, N., Sarpal, R., Trimble, W.S., and Brill, J.A. (2010). Stabilization of the actomyosin ring enables spermatocyte cytokinesis in Drosophila. Mol Biol Cell *21*, 1482-1493.
Greenspan, R.J. (1997). Fly Pushing: The Theory and Practice of Drosophila Genetics (CSHL Press).
Huang da, W., Sherman, B.T., and Lempicki, R.A. (2009). Systematic and integrative analysis of large gene lists using DAVID bioinformatics resources. Nat Protoc *4*, 44-57.
Ivanovska, I., Khandan, T., Ito, T., and Orr-Weaver, T.L. (2005). A histone code in meiosis: the histone kinase, NHK-1, is required for proper chromosomal architecture in Drosophila oocytes. Genes & development *19*, 2571-2582.
Ivanovska, I., Lee, E., Kwan, K.M., Fenger, D.D., and Orr-Weaver, T.L. (2004). The Drosophila MOS ortholog is not essential for meiosis. Current biology : CB *14*, 75-80.
Kashevsky, H., Wallace, J.A., Reed, B.H., Lai, C., Hayashi-Hagihara, A., and Orr-Weaver, T.L. (2002). The anaphase promoting complex/cyclosome is required during development for modified cell cycles. Proceedings of the National Academy of Sciences of the United States of America *99*, 11217-11222.
Lee, L.A., Van Hoewyk, D., and Orr-Weaver, T.L. (2003). The Drosophila cell cycle kinase PAN GU forms an active complex with PLUTONIUM and GNU to regulate embryonic divisions. Genes & Dev *17*, 2979-2991.

Preuss, F., Fan, J.Y., Kalive, M., Bao, S., Schuenemann, E., Bjes, E.S., and Price, J.L. (2004). Drosophila doubletime mutations which either shorten or lengthen the period of circadian rhythms decrease the protein kinase activity of casein kinase I. Molecular and cellular biology *24*, 886-898.
Reed, B.H., and Orr-Weaver, T.L. (1997). The Drosophila gene morula inhibits mitotic functions in the endo cell cycle and the mitotic cell cycle. Development *124*, 3543-3553.
Schwanhausser, B., Busse, D., Li, N., Dittmar, G., Schuchhardt, J., Wolf, J., Chen, W., and Selbach, M. (2011). Global quantification of mammalian gene expression control. Nature *473*, 337-342.
Shamanski, F.L., and Orr-Weaver, T.L. (1991). The Drosophila plutonium and pan gu genes regulate entry into S phase at fertilization. Cell *66*, 1289-1300.
Subtelny, A.O., Eichhorn, S.W., Chen, G.R., Sive, H., and Bartel, D.P. (2014). Poly(A)-tail profiling reveals an embryonic switch in translational control. Nature *508*, 66-71.
Temme, C., Zaessinger, S., Meyer, S., Simonelig, M., and Wahle, E. (2004). A complex containing the CCR4 and CAF1 proteins is involved in mRNA deadenylation in Drosophila. The EMBO journal *23*, 2862-2871.
Westwood, J.T., Clos, J., and Wu, C. (1991). Stress-induced oligomerization and chromosomal relocalization of heat-shock factor. Nature *353*, 822-827.
Whittaker, A.J., Royzman, I., and Orr-Weaver, T.L. (2000). Drosophila double parked: a conserved, essential replication protein that colocalizes with the origin recognition complex and links DNA replication with mitosis and the down-regulation of S phase transcripts. Genes & development *14*, 1765-1776.
Wisniewski, J.R., Zougman, A., Nagaraj, N., and Mann, M. (2009). Universal sample preparation method for proteome analysis. Nat Methods *6*, 359-362.
Xiang, Y., Takeo, S., Florens, L., Hughes, S.E., Huo, L.J., Gilliland, W.D., Swanson, S.K., Teeter, K., Schwartz, J.W., Washburn, M.P*., et al.* (2007). The inhibition of polo kinase by matrimony maintains G2 arrest in the meiotic cell cycle. PLoS Biol *5*, e323.